Journal of
Ceramic Science
and Technology

J. Ceram. Sci. Tech., 02 [02] 97-102 (2011)
DOI: 10.4416/JCST2011-00008
available online at: http://www.ceramic-science.com

Photoactive TiO_2 Nanopowder Synthesized at Low Temperature without a Catalyst

J.-P. Nikkanen*[1], E. Huttunen-Saarivirta[1], T. Kanerva[1], V. Pore[2], T. Kivelä[2], E. Levänen[1], T. Mäntylä[1]

[1]Tampere University of Technology, Department of Materials Science, P. O. Box 589, FIN-33101 Tampere, Finland
[2]University of Helsinki, Department of Chemistry, P.O. Box 55, FI00014 Helsinki, Finland
received February 14, 2011; received in revised form March 6, 2011; accepted March 14, 2011

Abstract

Nanocrystalline titanium dioxide (TiO_2) anatase powder was synthesized at 50 °C under normal pressure using the sol-gel method without a base or acid catalyst. The structural and photocatalytic properties of the produced anatase powder were determined with X-ray diffraction, transmission electron microscopy and nitrogen adsorption testing, and compared to those of anatase powder synthesized in a conventional process by calcining at 450 °C. The photocatalytic activity was confirmed with methylene blue (MB) discoloration tests.

The obtained results showed that the crystal size of anatase produced with the low-temperature catalyst-free method averaged 5.5 nm, while it was 12 nm for the anatase made by calcining. As a consequence, the specific surface area of the anatase powder synthesized at low temperature was three times higher than that of the calcined powder. The weight-based photocatalytic activity of the low-temperature-synthesized powder was 2.5 times higher than that of calcined powder. Therefore, the activity per unit of surface area was slightly higher for calcined anatase.

Keywords: Sol-gel processes, titanium dioxide, anatase, grain growth, calcination

I. Introduction

Titanium dioxide (TiO_2) is widely used in antifogging glasses and self-cleaning surfaces because of its photocatalytic activity [1,2]. Nanocrystalline titanium dioxide is of particular interest for applications in solar cells [3,4] and lithium batteries [5]. It has been also tested for the photodegradation of many organic compounds such as poly(bisphenol-A-carbonate) [6], or, for example, various dyes like methyl orange [7], methylene blue [8] and *p*-nitrophenol [9].

Numerous methods have been employed to achieve a controlled formation of crystalline TiO_2 nanoparticles. Promising techniques are, for example, liquid flame spraying (LFS) [10] and sol-gel synthesis based on alkoxide (M-OR) precursors. In the latter, metal alkoxides are dissolved into an organic solvent to be followed by reactions with water. When controlled hydrolysis and condensation reactions are realized, the hydroxyl ion attaches to the metal atom of the alkoxide and disconnects the alkyl group of the compound. The hydrolysis occurs as a result of reaction (1) [11–13]:

$$M-OR + H_2O \rightarrow M-OH + ROH \quad (1)$$

In the next step, the partially hydrolyzed molecules undergo a condensation reaction between OH groups, liberating either a water molecule (oxolation, reaction 2) [11–13]:

$$M-OH + OH-M \rightarrow M-O-M + H_2O \quad (2)$$

or alcohol (alkoxolation, reaction 3) [11–13]:

$$M-OH + OR-M \rightarrow M-O-M + ROH \quad (3)$$

When titanium dioxide is synthesized by a sol-gel route, hydrolysis and condensation reactions are followed by the formation of (TiO_6^{2-}) octahedra. The final structure of TiO_2 depends on how these octahedra are linked to each other. In the case of anatase, the primary connection of (TiO_6^{2-}) octahedra has been reported to be edge sharing, as shown in Fig. 1 [11, 12].

Conventionally, sol-gel reactions are catalyzed by acids or bases and the produced powders are non-crystalline in structure. Heat treatment of the synthesized particles has been reported to increase the particle size and to decrease the specific surface area [14]. To keep the particle size small, modified methods to prepare crystalline titanium dioxide have been applied [11, 12, 15, 16]. In these studies, hydrolysis and condensation and thus the morphology of final product are affected by catalysts or by using the temperature as a variable in the hydrothermal synthesis.

Unlike in previous studies, in this study, crystalline titanium dioxide nanoparticles were synthesized at a constant temperature of 50 °C without any catalyst. The specific surface area, particle size and presumed crystallization path of the anatase synthesized without catalyst were compared to calcined reference anatase. The photocatalytic activity was confirmed in methylene blue (MB) discoloration tests.

* Corresponding author: juha-pekka.nikkanen@tut.fi

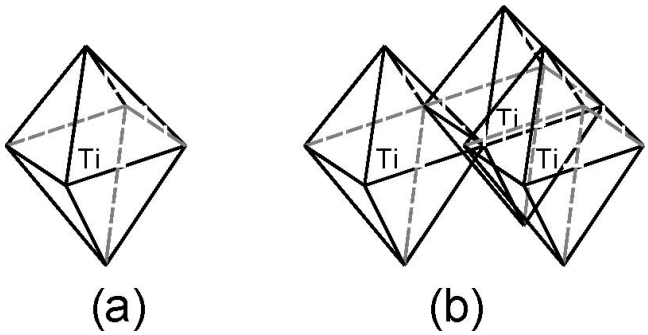

Fig. 1: TiO_6^{2-} octahedra (a) and the elemental structure of anatase (b).

In this study, we verify that the specific surface area of titanium dioxide depends on the synthesis method and the photocatalytic activity depends on the specific surface area. The aim of this study is to identify photocatalytic properties of low-temperature-synthesized titanium dioxide and also to compare the characteristics of anatase synthesized at low temperature with those of the calcined reference sample.

II. Experimental Details

(1) Synthesis of TiO_2 powders

Nanosized TiO_2 powder was prepared by hydrolysis and condensation reaction of titanium alkoxide. At the beginning, 1.875 ml tetra-n-butyl orthotitanate ($C_{16}H_{36}O_4Ti$ > 98 %, VWR) was dissolved in 6.25 ml of 2-propanol (C_3H_7OH > 99.5 VWR, amount of water ≥ 0.2 %). The solution mixture was stirred for 15 min and then 90 ml of ion-exchanged water was added into the solution container. After mixing for 3 min, half of the solution was separated to another container, filtered and dried in an oven at 50 °C for 12 h. A small amount of dried powder was stored for examination and the rest of it was calcined at 450 °C for 1 h and used as a reference. The other half of the solution was further stirred in a sealed reflux condensed reaction vessel for 24 h. The temperature of the solution was 50 °C and relative humidity inside the vessel 98 % (measured with a Lambrecht 235 hygrometer). Finally, the precipitates were filtered and dried in an oven at 50 °C for 12 h. The synthesis procedure is described schematically in Fig. 2.

(2) Characterization

The crystal structure of TiO_2 powders was determined with a Siemens Kristalloflex D-500 X-ray diffractometer and monocromatized CuKa radiation. The crystal sizes were estimated from XRD-patterns, using a Scherrer formula $t = (0.9\,\lambda/B\,\cos\theta)$ [17], where t is the size in nm, λ is the wavelength of X-rays in Å (1.5418 Å), B is full width half maxima of the peak in radians and θ is the Bragg angle. The morphology and the size of particles were determined with a JEOL, JEM 2010 transmission electron microscope and acceleration voltage of 200 kV. The particle size was determined by measuring 700 particles from several TEM micrographs. The specific surface area of powders was measured in a nitrogen adsorption test using a Brunauer-Emmett-Teller (BET) method and a Coulter Omnisorp 100 cx device. Here the average size of the particles was calculated by using the following equation: $d_{BET} = 6/(\varrho S_{ssa})$, where ϱ is the density and S_{ssa} is the specific surface area.

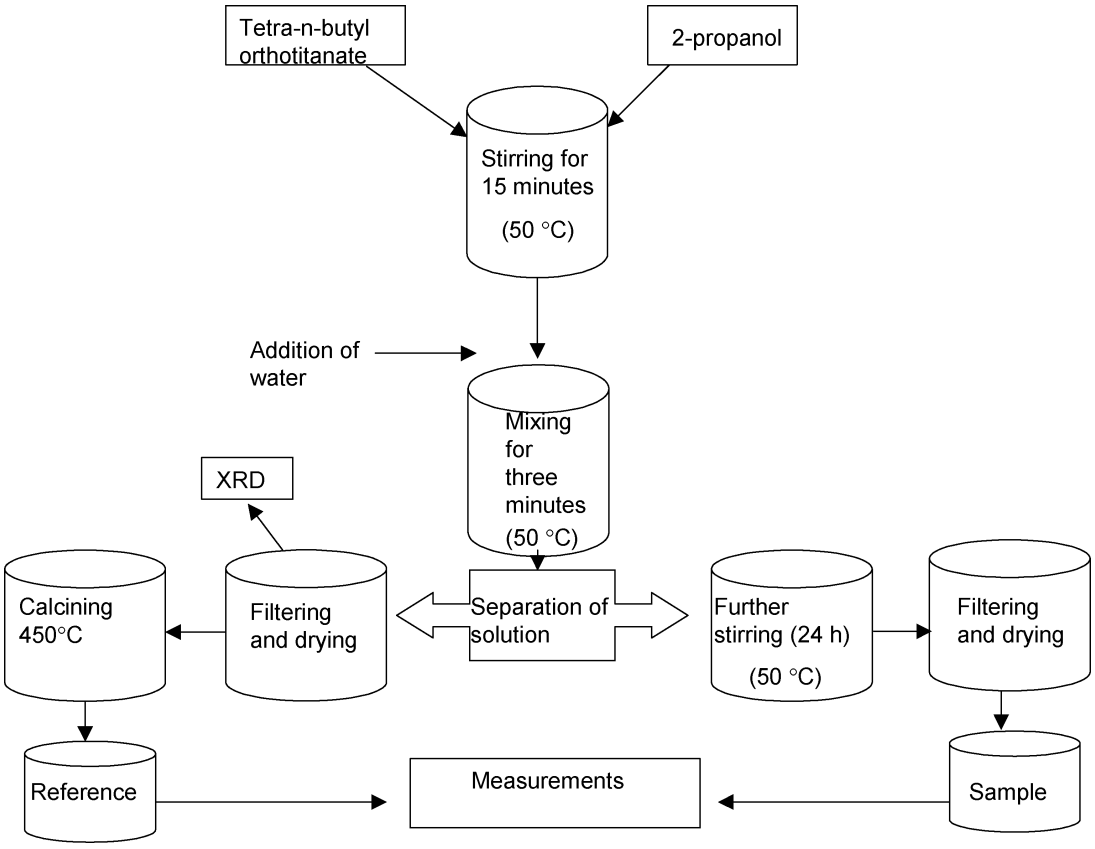

Fig. 2: Flow sheet for the preparation of TiO_2 samples.

(3) Photocatalytic measurements

Photocatalytic measurements were performed in an aqueous solution of methylene blue (MB). 10 mg of each TiO_2 powder was dispersed into 100 ml of 0.03 mM MB solution in an open beaker and the dispersion was magnetically stirred during the whole experiment. It should be emphasized that in order to correlate the specific surface area and photocatalytic activity, an equal mass of the low-temperature-synthesized powder and calcined reference was used. The photocatalytic activity of both powders was also expressed with respect to the surface areas.

In order to reach adsorption equilibrium, the dispersions were first kept in the dark for 30 min after which the UV lamp was turned on. The dispersions were illuminated from above with a 20-W Sylvania Blacklight Blue UV-lamp (peak maximum at 356 nm, intensity ~ 0.8 mW/cm^2). The concentration of methylene blue in the solution was followed with UV-VIS spectroscopy (HP 8453 spectrophotometer). At 1-h intervals, 3 ml of dispersion was taken and centrifuged, to separate the photocatalyst particles from the solution. After this, the absorbance of MB at the wavelength of 665 nm was measured. A dark experiment without any irradiation but under otherwise identical conditions was conducted for comparison.

III. Results and Discussion

Fig. 3 shows the XRD-patterns from the samples. The curve (a) illustrates an amorphous structure of the powder dried after only three minutes of mixing. The anatase phase is detected in the synthesized powder (b) and in the calcined reference powder (c). The diffraction peaks of the powder synthesized at low temperature are broader than the peaks in the calcined powder. This is related to a smaller crystal size in the sample prepared at low temperature as compared to the reference. The main reason for this is the absence of the grain growth at low temperature. Determined with the Scherrer formula, the crystallite sizes were 5.5 nm for the low-temperature-synthesized powder and 12 nm for the reference.

Transmission electron micrographs of the powders are shown in Fig. 4. The micrographs confirm the dependence of the particle size on the preparation method. The finding that grain growth occurs during the calcining, which was detected in XRD curves (Fig. 3), is also observed in the TEM micrographs (Fig. 4). This observation is also consistent with the literature: grain growth and densification of the agglomerates of TiO_2 powder have been reported to occur during heat treatment [11, 15, 16]. At low temperature, the grain growth is insignificant, but some agglomeration has occurred, as can be seen in Fig. 4. The average size of discrete TiO_2 particles was measured using TEM micrographs. These measurements showed average diameters to be 5.6 and 12.5 nm for the low- temperature-synthesized particles and for the reference, respectively. The particle size distributions, also determined from TEM micrographs, are shown in Fig. 5.

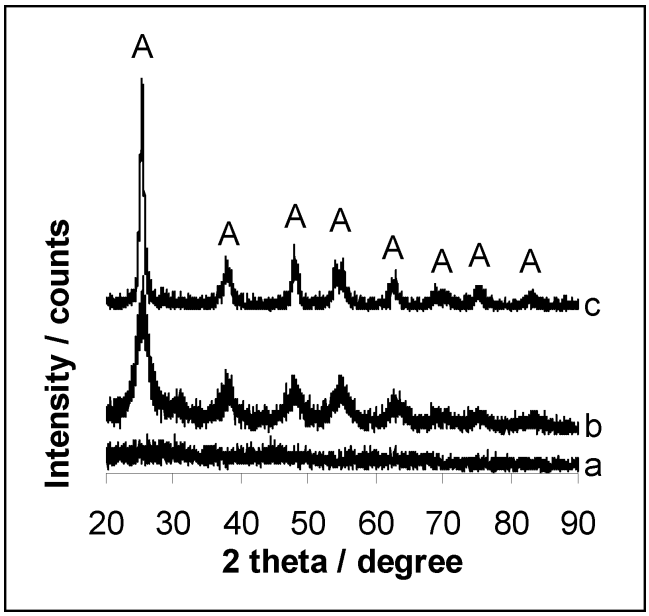

Fig. 3: XRD patterns of prepared powders: (a) non-crystalline, (b) low-temperature-synthesized and, (c) calcined TiO_2 sample. A: anatase.

The BET measurements were performed to determine the specific surface areas of the powders. It also offered a third way to measure the particle size of powders in this study. The specific surface areas measured 271 and 86 m^2/g for the low-temperature-synthesized powder and for the reference, respectively. The difference between the specific surface areas for the powders is roughly threefold. The average particle sizes (d_{BET}) calculated from the specific surface areaswere 6.0 and 18 nm for the low-temperature-synthesized powder and for the calcined reference, respectively. It should be emphasized that the calculated particle size d_{BET} is larger for the calcined reference than the crystal size d_{XRD}, which indicates the hard agglomeration of calcined crystallites.

(1) Suggested precipitation mechanism of the TiO_2

Addition of water into the solution of tetra-n-butyl orthotitanate and 2-propanol caused the formation of the white precipitate in the reaction vessel. This is due to the fast hydrolysis and condensation reactions of alkoxide, nucleation of (TiO_6^{2-}) octahedra and, further the aggregation of these octahedra. Hydrolysis is followed by the condensation of the hydrolyzed species. In next step follows the nucleation of the octahedra (TiO_6^{2-})[11]. These octahedra aggregate and, because of that, form the precipitate. The precipitate is non-crystalline as was characterized with XRD (Fig. 3 a). After the fast formation of precipitate, the precipitate undergoes slow peptization [18]. In peptization, the original bonds of the amorphous particles are broken and (TiO_6^{2-}) octahedral are released. Concurrently with peptization process, reaggregation occurs in the solution, and isolated octahedra connect together. The crystal structures of titanium dioxide consist of (TiO_6^{2-}) octahedra so that the overall stoichiometry is TiO_2. The formation of anatase requires a minimum of three octahedra to connect to each other with shared edges (Fig. 6) [11, 12, 18].

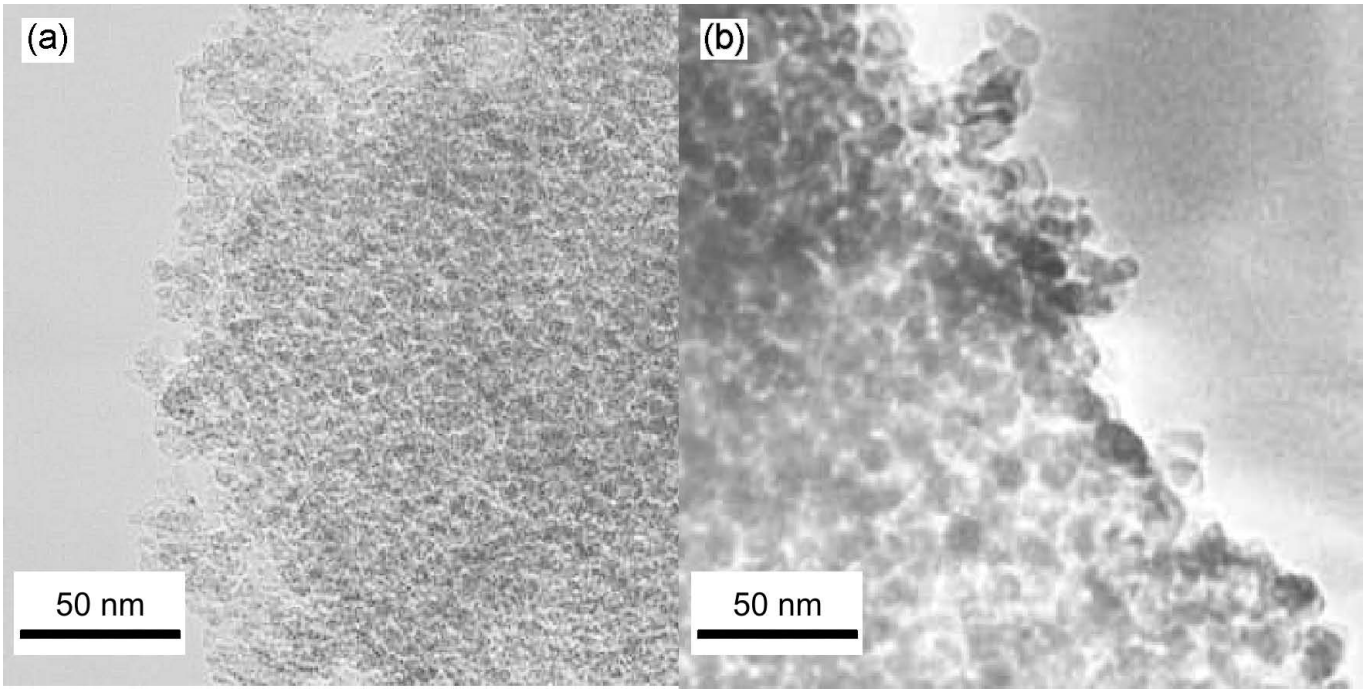

Fig. 4: TEM micrographs of samples synthesized at low temperature (a) and the calcined reference sample (b).

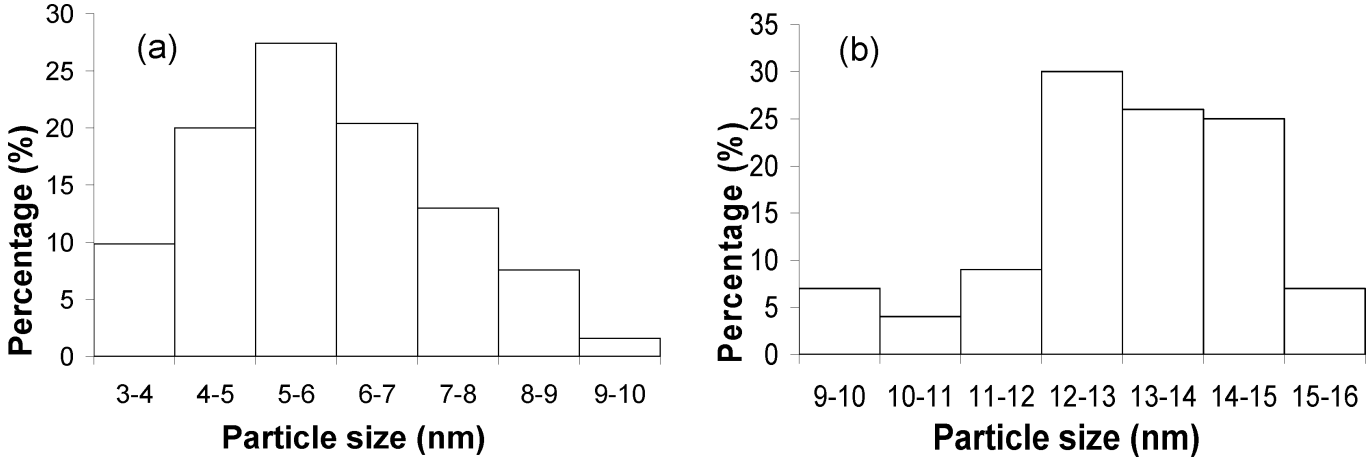

Fig. 5: Particle size distribution (nm) of samples synthesized at low temperature (a) and the calcined reference sample (b), n = 700.

(2) Photocatalytic discoloration of MB

The experimental results of photocatalytic discoloration of MB with low-temperature-synthesized powder and reference powder are shown in Table 1. The dark experiment shows that there is no significant adsorption of MB on the synthesized sample. On the contrary, the concentration of MB slightly increased during a 4-h experiment. The reason for this is probably the evaporation of water from the open beaker. In a test using UV-radiation, the concentration of MB began to decrease immediately after the UV-lamp was switched on, particularly in the case of the low-temperature-synthesized powder. After 4 h of radiation about 30 % of MB was degraded. The photocatalytic activity of the reference powder was much lower. During the first hour, no significant photoactivity was observed. This was mainly because of a strong agglomeration of the particles. After 1 h of vigorous stirring, the concentration of MB started to decrease. The final MB concentration of the reference after 4 h of irradiation was decreased by about 12 %. The photocatalytic discoloration of MB was 2.5-fold with the low-temperature-synthesized sample.

The most significant difference between the low-temperature-synthesized sample and the reference is in the particle size, resulting in the differences in their specific surface areas. TiO_2 photocatalysis is based on absorption of the efficient photon ($h\nu \geq E_G = 3.2$ eV) by titania, electron-hole formation and subsequent oxidation and reduction reactions on the surfaces of TiO_2 [19]. A requirement for the efficient degradation of the organic compound by the photocatalysis is the contact of the organic molecule and TiO_2. The surfaces of the nanosized TiO_2 were found to play the main role during photocatalytic discoloration of methylene blue because of the specific structural species placed on the surfaces of the nanoparticles [20].

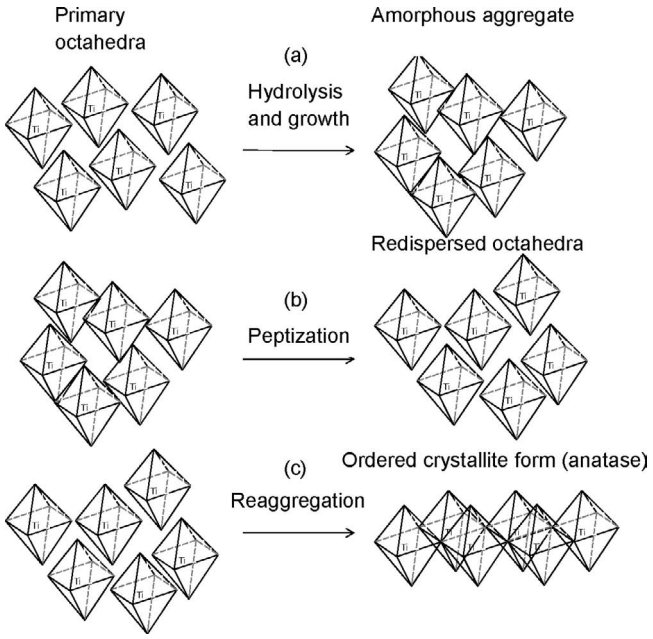

Fig. 6: Suggested mechanism for the formation of anatase without a catalyst.

In this study, there is good correlation between 3-fold specific surface area and 2.5-fold photocatalytic activity. However, the relative discoloration of MB expressed per unit of surface area (m^2) during 4-h experiment is $1.1\times10^{-3}\,m^2)^{-1}$ for the low-temperature-synthesized sample and $1.4\times10^{-3}\,(m^2)^{-1}$ for the reference powder (Table 1). These activities are reasonably close to each other. The slightly higher activity/surface area of the reference powder may be the result of many reasons. One possible reason is that there are more photoactive sites/surface area [20] in the reference powder than in the powder synthesized at low temperature. Second possible reason is the better adsorption ability for hydroxyl ions on the surfaces of the reference powder than on the surfaces of the low-temperature-synthesized powder. Thirdly, the quantum efficiency of the synthesized powders can differ from each other.

Table 1: Photocatalytic discoloration of MB as a function of irradiation over time. RD is the relative discoloration of MB expressed per unit of surface area (m^2) during a 4-h experiment.

Time (min.)	Sample + UV C/C_0	Reference + UV C/C_0	Sample in dark C/C_0
0	1	1	1
60	0.94	1.01	1.08
120	0.83	0.95	1.08
180	0.77	0.91	1.08
240	0.70	0.88	1.11
240	RD $1.1\times10^{-3}(m^2)^{-1}$	RD $1.4\times10^{-3}(m^2)^{-1}$	

However, we have clearly shown that the specific surface area of titanium dioxide depends on the synthesis method and photocatalytic activity depends on the specific surface area. For that reason, the essential aim in the development of more effective photocatalytic titanium dioxide is to decrease the particle size to increase the surface area of the photocatalyst.

IV. Conclusions

Crystalline anatase TiO_2 was prepared in a low-temperature synthesis without a catalyst, and its structure and properties were compared to those of anatase powder produced with a conventional calcination method. The crystal structure, particle size, specific surface area and the photocatalytic activity results show that the low-temperature-synthesized powder has a small grain size, high specific surface area and increased activity as a result.

The formation of anatase in the nanocolloidal solution is a multiple-step process: the first step is the formation of amorphous precipitates by fast hydrolysis and condensation. In the next step, the amorphous agglomerates undergo slow peptization, and finally the crystalline structure is formed by reaggregation of the primary octahedra.

It was observed that the final crystal size of the low-temperature-synthesized anatase sample is approximately 5.5 nm, while it is about 12 nm for the calcined sample. As a consequence, the specific surface area of the low-temperature powder is 271 m^2/g, and 86 m^2/g for reference powder. The over threefold difference between the surface areas can be explained by the absence of the grain growth at low temperature.

The low-temperature-synthesized powder showed 2.5-fold photocatalytic activity in the discoloration measurements of MB compared to the calcined reference powder. This is due to the higher functional surface area of the low-temperature-synthesized powder than that of the reference.

Acknowledgements:

The present study was partly supported by The Finnish National Graduate School on New Materials and Processes.

References

1 Watanabe, T., Nakajima, A., Wang, R., Minabe, M., Koizumi, S., Fujishima, A., Hashimoto, K.: Photocatalytic activity and photoinduced hydrophilicity of titanium dioxide coated glass, *Thin Solid Films*, **351**, 260–263, (1999).

2 Fujishima, A., Hashimoto, K., Watanabe, T.: Photocatalysis Fundamentals and Applications, BKC, Tokyo, (1999).

3 Nazeeruddin, M.K., Kay, A., Rodicio, I., Humphry-Baker, R., Mueller, E., Liska, P., Vlachopoulos, N., Grätzel, M.: Conversion of Light to Electricity by *cis*-X_2Bis(2,2'-bibyridyl-4,4'-dicarboxylate)ruthenium(II) Charge-Transfer Sensitizers (X= Cl^-, Br^-, I^-, CN^-, and SCN^-) on Nanocrystalline TiO_2 Electrodes, *J. Am. Chem. Soc.*, **115**, 6382–6390, (1993).

4 Hagfeldt, A., Grätzel, M.: Light-Induced Redox Reactions in Nanocrystalline Systems, *Chem. Rev.*, **95**, 49–68, (1995).

5 Exnar, I., Kavan, L., Huang, S.Y., Grätzel, M.: Novel 2 V rocking-chair lithium battery based on nano-crystalline titanium dioxide, *J. Power. Sources*, **68**, 720–722, (1997).

6 Sivalingam, G., Madras, G.: Photocatalytic degradation of poly(bisphenol-A-carbonate) in solution over combustion-synthesized TiO_2: mechanism and kinetics, *Appl. Catal. A: General*, **269**, 81–90, (2004).

7 Wang, Z., Jiang, T., Du, Y., Chen, K., Yin, H.: Synthesis of mesoporous titania and the photocatalytic activity for decomposition of methyl orange, *Mater. Lett.*, **60**, 2493–2496, (2006).

[8] Nagaveni, K., Sivalingam G., Hedge M.S., Madras, G.: Solar photocatalytic degradation of dyes: high activity of combustion synthesized nano TiO_2, *Appl. Catal. B: Environmental*, **48**, 83 – 93, (2004).

[9] Hong S.-S., Lee M.S., Ju C.-S., Lee G.-D., Park S.S., Lim K.-T.: Photocatalytic decomposition of *p*-nitrophenol over titanium dioxides prepared in water-in-carbon dioxide microemulsion, *Catal. Today*, **93**, 871 – 876, (2004).

[10] Aromaa, M., Keskinen, H., Mäkelä, J.M..: The effect of process parameters at the Liquid Flame Spray generated titania nanoparticles, *Biomol. Eng.,* **24**, 543 – 548, (2007).

[11] Gobal, M., Moberly Chan, W.J., De Jonghe, L.C.: Room temperature synthesis of crystalline metal oxides, *J. Mater. Sci.*, **32**, 6001 – 6008, (1997).

[12] Watson, S., Beydoun, D., Scott, J., Amal, R.: Preparation of nanosized crystalline TiO_2 particles at low temperature for photocatalysis, *J. Nanopart. Res.*,**6**, 193 – 207, (2004).

[13] Brinker, C.J., Scherer, G.W.: Sol-Gel Science: The Physics and Chemistry of Sol-Gel Processing, AP, San Diego, (1990).

[14] Wang, C.-C., Ying, J.Y.: Sol-Gel Synthesis and Hydrothermal Processing of Anastase and Rutile Titania Nanocrystals, *Chem. Mater.*, **11**, 3113 – 3120, (1999).

[15] Tang, Z., Zhang, J., Cheng, Z., Zhang, Z.: Synthesis of nanosized rutile TiO_2 powder at low temperature, *Mater. Chem. Phys.*, **77**, 314 – 317, (2002).

[16] Nikkanen, J.-P., Kanerva, T., Mäntylä, T.: The effect of acidity in low-temperature-synthesis of titanium dioxide, *J. Cryst. Growth*, **304**,179 – 183, (2007).

[17] Cullity, B.D.: Elements of X-ray Diffraction, Addison-Wesley Publishing Company Inc., USA, (1967).

[18] Vorkapic, D., Matsoukas, T.: Effect of Temperature and Alcohols in the Preparation of Titania Nanoparticles from Alkoxides, *J. Am. Ceram. Soc.*, **81**, 2815 – 2820, (1998).

[19] Houas, A., Lachheb, H., Ksibi, M., Elaloui, E., Guillard, C., Herrmann, J.M.: Photocatalytic degradation pathway of methylene blue in water, *Appl. Catal. B: Environmental*, **31**, 145 – 157, (2001).

[20] Hsiung, T.L., Wang, H.P., Lin, H.P.: Chemical structure of photocatalytic active sites in nanosize TiO_2, *J. Phys. Chem. Solids*, **69**, 383 – 385, (2008).